

1           **XPS and NRA depth profiling of nitrogen and carbon simultaneously**  
2           **implanted into copper to synthesize C<sub>3</sub>N<sub>4</sub> like compounds**

3                           **J. L. Colaux<sup>1</sup>, P. Louette<sup>2</sup>, G. Terwagne<sup>1</sup>**

4                           Research center in Physics of Matter and Radiation (PMR),

5                           <sup>1</sup>Laboratoire d'Analyses par Réactions Nucléaires (LARN),

6                           <sup>2</sup>Laboratoire Interdisciplinaire de Spectroscopie Electronique (LISE),

7                           University of Namur (FUNDP),

8                           61 Rue de Bruxelles, B - 5000 Namur

9  
10       **Abstract**

11           Carbon nitride nano-compounds have been synthesized into copper by simultaneous  
12 high fluence ( $10^{18}$  at.cm<sup>-2</sup>) implantation of <sup>13</sup>C and <sup>14</sup>N ions. The implantations were  
13 performed with a 2 MV Tandem accelerator. The terminal voltage was fixed at 400 kV and  
14 the target temperature was maintained at 250 °C during the process. Depth profiling of <sup>13</sup>C  
15 and <sup>14</sup>N has been performed using (d,p) and (d,α) nuclear reactions induced by a 1.05 MeV  
16 deuteron beam. The retained dose deduced from NRA measurement is relatively close to the  
17 implanted one, which indicates that carbon and nitrogen diffusion processes were likely  
18 limited during implantation.

19           The chemical bonds between carbon and nitrogen were studied as a function of depth by  
20 X-ray photoelectron spectroscopy (XPS). The C 1s and N 1s core level photoelectron spectra  
21 revealed the presence of different types of C-N bonds, which correspond to specific kinds of  
22 chemical states. These results indicate that different carbon nitride compounds have been  
23 formed during the implantation.

24 PACS codes : 25.45.De, 29.30.Ep, 79.60.i, 81.07.b

25 Keywords: Carbon, Nitrogen, XPS, NRA, Implantation

26 Corresponding author: J. L. Colaux, FUNDP, 61 rue de Bruxelles, B-5000 Namur, Belgium

27                           E-mail: julien.colaux@fundp.ac.be

28                           Phone: 32 (0) 81 72 54 79

29                           Fax: 32 (0) 81 72 54 74

## 1 **1. Introduction**

2

3 In recent years, the synthesis of crystalline carbon nitrides has been extensively  
4 investigated as they are expected to show remarkable physical properties such as high  
5 hardness and wear resistance. A wide variety of elaboration techniques have been used such  
6 as reactive sputtering, chemical vapour deposition, pyrolysis of organic materials, laser  
7 deposition and ion implantation [1-6]. The fully crystalline phase formation remains  
8 nevertheless very difficult to achieve, whatever the technique employed. However, even  
9 amorphous carbon nitride layers may have suitable physical properties for the use in many  
10 tribological applications, for instance as protective coatings.

11 The aim of our study is to synthesize homogeneous, reproducible and well characterized  
12 carbon nitride compounds by means of ion implantation. For that purpose we performed  
13 simultaneous implantations of  $^{13}\text{C}$  and  $^{14}\text{N}$  into copper at 250 °C. Carbon and nitrogen depth  
14 distributions were determined by non resonant nuclear reactions induced by a 1.05 MeV  
15 deuteron beam. Then, the chemical bonds between carbon and nitrogen implanted atoms were  
16 studied by XPS measurements.

17

## 18 **2. Experimental**

19

### 20 **2.1 Materials and substrate implantation**

21 The samples are polished polycrystalline copper substrates. Simultaneous  $^{13}\text{C}$  and  $^{14}\text{N}$   
22 implantations were performed using the non deflected beam line of the 2 MV ALTAÏS<sup>1</sup>  
23 Tandatron accelerator installed at LARN. We used a cesium sputter ion source (Snics) to  
24 perform these implantations. A copper cathode filled with a mixture of  $\text{K}^{13}\text{C}^{14}\text{N}$  (30 mg) and

---

<sup>1</sup>Accélérateur Linéaire Tandatron pour l'Analyse et l'Implantation des Solides

1 Ag (60 mg) is bombarded by a  $\text{Cs}^+$  ion beam.  $\text{CN}^-$  anions are sputtered from the cathode and  
2 accelerated in the low energy part of the Tandetron accelerator. Passing through the stripper  
3 canal, the  $\text{CN}^-$  anions hit  $\text{N}_2$  gas molecules and a large variety of  $\text{CN}^+$ ,  $\text{C}^{n+}$  and  $\text{N}^{q+}$  cations are  
4 produced and accelerated in the high energy part of Tandetron accelerator towards the copper  
5 sample. The sample was maintained at  $250\text{ }^\circ\text{C}$  and the vacuum pressure did not exceed  
6  $10^{-5}$  Pa during the implantation procedure. The terminal voltage of the accelerator was fixed at  
7 400 kV, which gives for instance energies of respectively 608 keV and 625 keV for  $^{13}\text{C}^+$  and  
8  $^{14}\text{N}^+$  (Table 1). The current density of the ion beam was measured around  $80\text{ }\mu\text{A}\cdot\text{cm}^{-2}$  and the  
9 total fluence was about  $10^{18}$  at. $\text{cm}^{-2}$  over an area of 3 mm in diameter.

10

## 11 **2.2 Nuclear reactions and X-Ray photoelectron characterizations**

12 The depth distributions of carbon and nitrogen in copper were studied using (d,p) and  
13 (d, $\alpha$ ) non resonant nuclear reactions induced on  $^{13}\text{C}$  and  $^{14}\text{N}$ . The experimental set-up used to  
14 perform these measurements was presented in a previous work [7].

15 XPS measurements were performed to study the composition and the nature of the  
16 carbon nitride compounds formed in the implanted copper sample. XPS spectra were recorded  
17 with a SSX 100 Spectrometer system (Surface Science Instrument) equipped with a  
18 hemispherical electron analyser. All reported spectra were recorded at a  $35^\circ$  take-off angle  
19 relative to the substrate using monochromatized Al  $\text{K}_\alpha$  radiation as excitation source  
20 (1486.6 eV). Nominal resolution was measured as full width at half maximum of respectively  
21 0.92 and 1.4 eV for core-levels and survey spectra of the Au  $4f_{7/2}$  peak. The argon ion gun  
22 used for sputtering was equipped with a special regulating system which enabled automated  
23 long time depth profile procedures. A depth profile procedure consists of several cycles of  
24 recording different XPS peaks followed by etching the sample. The recorded XPS peaks and  
25 the etching time have to be fixed before running the procedure and can not be changed during

1 its execution. All XPS procedures were performed with an ion beam raster size of about  
2  $2 \times 2 \text{ mm}^2$  and an  $\text{Ar}^+$  ion energy of 3.9 keV. The carbon and copper sputter rates obtained in  
3 these conditions were determined in order to convert the etching time in a metric scale (nm).  
4 For that purpose, a multilayer sample ( $\text{C}_{50 \text{ nm}} / \text{Cu}_{250 \text{ nm}} / \text{Si}$ ) was prepared by physical vapour  
5 deposition. The carbon and copper layers thicknesses were measured by a stylus profilometer  
6 from Veeco Instruments (Surface Profile Measuring System Dektak). We performed 40  
7 cycles to determine the depth profile of this sample. For each cycle, the C 1s, Cu  $2p_{3/2}$  and  
8 Si 2p signals were recorded and the etching time was fixed to 60 s. The chemical composition  
9 was obtained from the areas of the detected XPS peaks, performing Shirley background  
10 subtraction and taking into account sensitivity factors for each constituent. In the same way,  
11 28 cycles were performed to characterize the implanted samples. In this case the C 1s, N 1s,  
12 O 1s and Cu  $2p_{3/2}$  peaks were studied, and the etching time was fixed to 120 s. Moreover, the  
13 spectra were referenced to the Cu  $2p_{3/2}$  metallic copper line, always present in the sample, set  
14 at binding energy of 932.7 eV. The peaks were analysed using mixed Gaussian–Lorentzian  
15 curves (with a 70 % Gaussian content). Binding state information was determined from  
16 chemical shifts observed on the binding energy scale after the curve fitting of XPS peaks.

17

### 18 **3. Results and discussion**

19

20 We first present NRA results from carbon and nitrogen nuclear reactions obtained with  
21 the 1.05 MeV deuteron beam. Then, we discuss the procedure applied to convert the XPS  
22 sputtering time into the depth scale. The formation of characteristic carbon nitrogen bonds  
23 within the implanted layer is discussed on the basis of XPS measurements.

24

1 Figure 1 shows the experimental spectrum recorded at 150° (NRA detector) for the  
2 sample simultaneously implanted with  $^{13}\text{C}$  and  $^{14}\text{N}$  at 250 °C. The peak labelled  $^{13}\text{C}_{\text{p}0}$   
3 observed just below 6.0 MeV is due to the  $^{13}\text{C}(\text{d},\text{p}_0)^{14}\text{C}$  nuclear reaction. The very intense  
4 peak labelled  $^{12}\text{C}_{\text{p}0}$  is attributed to  $^{12}\text{C}$  surface contamination occurring during the  
5 implantation process. All other peaks are assigned to  $^{14}\text{N}(\text{d},\text{p}_i)^{15}\text{N}$  (with  $i = 0, 1, 2, 3, 4$  or  $5$ )  
6 and  $^{14}\text{N}(\text{d},\alpha_i)^{12}\text{C}$  (with  $i = 0$  or  $1$ ) nuclear reactions. The simulation was performed with the  
7 SIMNRA 6.04 program [8] using the nuclear reaction cross sections measured by M.  
8 Kokkoris et al. [9], S. Pellegrino et al. [10] and J.L. Colaux et al. [11]. The copper sample  
9 used in this program was subdivided into thin layers whose composition was adapted to adjust  
10 the simulated curve to the experimental spectrum. The simulated spectrum is represented by  
11 the solid line in Figure 1. The thickness of layers provide by the SIMNRA program is given in  
12  $\text{at.cm}^{-2}$ . The density of each layer was deduced from its composition in order to convert its  
13 thickness in a metric scale (nm). The calculated depth distributions of carbon (open circles)  
14 and nitrogen (open squares) are shown in Figure 2. A carbon surface contamination of about  
15 20 nm is clearly observed in Figure 2.a. This may be explained by some carbon build-up  
16 phenomena during implantation as no carbon is detected on the virgin sample surface. The  
17 carbon and nitrogen depth distributions may be decomposed into a combination of Gaussian  
18 curves assigned to the different implanted ion species [12]. This decomposition is not  
19 represented in Figure 2. Nevertheless the position of each Gaussian curve maximum is  
20 reported in Table 1. We can see good agreement between the projected ranges calculated with  
21 SRIM2003 code ( $R_{\text{SRIM}}$ ) [13] and the experimental results ( $R_{\text{exp}}$ ). The slight difference  
22 between  $R_{\text{SRIM}}$  and  $R_{\text{exp}}$  was discussed in a previous work [14]. Finally, converting the  
23 nanometric depth scale in a  $10^{15} \text{at.cm}^{-2}$  one, the integral of the depth profiles allows us to  
24 estimate the incorporated carbon and nitrogen atomic densities at  $5.0 \cdot 10^{17} \text{at.cm}^{-2}$  and  
25  $4.5 \cdot 10^{17} \text{at.cm}^{-2}$  respectively. The sum of both is very close to the total implanted fluence

1 which was  $1.0 \cdot 10^{18} \text{ at.cm}^{-2}$ . These results enable us to conclude that carbon and nitrogen  
2 diffusion is low during the implantation process.

3  
4 The XPS depth profile of the  $\text{C}_{50 \text{ nm}} / \text{Cu}_{250 \text{ nm}} / \text{Si}$  multilayered sample is presented in  
5 Figure 3. The very sharp interface between the carbon and copper layers proves that the  $\text{Ar}^+$   
6 ion gun and the analysis beam are well aligned. On the other hand, the interface between  
7 copper layer and substrate (Si) is much less sharp, which suggests that the XPS depth  
8 resolution decreases with increasing depth. This may be explained by the sample roughness  
9 induced by  $\text{Ar}^+$  ion bombardment increasing with the etching time. The carbon and copper  
10 sputter rates deduced from Figure 3 are  $5.8 \text{ nm.min}^{-1} (S_C)$  and  $18.2 \text{ nm.min}^{-1} (S_{Cu})$   
11 respectively. This large difference implicates that the total sputter rate of the implanted  
12 sample will change with depth because the carbon concentration varies strongly along the  
13 depth scale. In order to determine the equivalent width ( $W_{Eq}$ ) sputtered during one etching  
14 cycle we have considered the following equation:

$$15 \quad W_{Eq} = T \times (S_C \times A + S_{Cu} \times (1 - A)) \quad \text{Equation 1}$$

16 where T is the etching time and A is the atomic concentration of carbon measured in the  
17 previous cycle. Note that the nitrogen concentration is not taken into account in this equation  
18 because, as will be seen later, the major fraction of nitrogen appears as gas bubbles.  
19 Moreover, as the carbon and copper sputter rates are strongly correlated to the experimental  
20 etching conditions, the sputter rates  $S_C$  and  $S_{Cu}$  has to be measured before each XPS depth  
21 profile.

22 The N 1s core level photoelectron spectrum, acquired at 630 nm depth, is presented in  
23 Figure 4.a. Three components ( $N_1$ ,  $N_2$  and  $N_3$ ) can clearly be resolved for this spectrum.  
24 According to the literature [15-18], the  $N_1$  and  $N_2$  components (centered at 398.6 eV and  
25 400.6 eV) are related to the presence of C-N bonds. The  $N_1$  component (FWMH = 1.7 eV) is

1 assigned to nitriles ( $-\text{C}\equiv\text{N}$ ) and pyridine ( $\text{C}-\text{N}=\text{C}$ ) type bonds while  $\text{N}_2$  (FWMH = 1.8 eV) is  
2 attributed to  $\text{sp}^2$  C–N bonds. The  $\text{N}_4$  component (centered at 397.2 eV, FWHM = 1.7 eV) may  
3 be added in the low energy tail of  $\text{N}_1$  peak. This can presumably be assigned to the  $\text{C}_3\text{N}_4$   
4 structure. The exact position and intensity of this component is nevertheless uncertain because  
5 it strongly depends on the exact background fitting. Thus the presence of  $\text{C}_3\text{N}_4$  will be not  
6 discussed here. The much broader component  $\text{N}_3$  (centered at 404.1 eV, FWHM = 3.6 eV) is  
7 attributed to nitrogen gas molecules [19]. The precipitation of nitrogen in large gas bubbles  
8 during the implantation was already highlighted in a previous work [12].

9       The C 1s core level photoelectron spectrum, acquired at the same depth, is presented in  
10 Figure 4.b. The long tail towards higher binding energies indicates the presence of low  
11 quantities of C–N and C–O bonds due to the higher electronegativity of nitrogen and oxygen.  
12 Nevertheless no clear peak components can be easily distinguished. To achieve the curve  
13 fitting, five components have been used. The major component  $\text{C}_0$  (centered at 284.4 eV,  
14 FWHM = 1.8 eV) corresponds to carbon atoms bonded to carbon neighbours, as graphite ( $\text{sp}^2$ )  
15 or amorphous ( $\text{sp}^3$ ) carbon. The  $\text{C}_1$  (centered at 286.3 eV, FWHM = 1.6 eV) and  $\text{C}_2$  (centered  
16 at 285.8 eV, FWHM = 1.5 eV) are related to nitrogen presence.  $\text{C}_1$  is assigned to nitriles  
17 ( $-\text{C}\equiv\text{N}$ ) and pyridine ( $\text{C}-\text{N}=\text{C}$ ) type bonds while  $\text{C}_2$  is attributed to  $\text{sp}^2$  C–N bonds [15-18].  
18 As these positions are very close, the following constraint was imposed on the  $\text{C}_1$  and  $\text{C}_2$   
19 areas to perform the curve fitting:

$$20 \quad 0.90 \times B(\text{N}_i) \leq A(\text{C}_i) \leq 1.10 \times B(\text{N}_i) \quad \text{for } i = 1 \text{ or } 2$$

21 where  $A(\text{C}_i)$  is the peak area of component  $\text{C}_i$  and  $B(\text{N}_i)$  is the peak area of the component  $\text{N}_i$   
22 normalized by the sensitivity factor of nitrogen.  $\text{C}_3$  (centered at 288.0 eV) is attributed to the  
23 C–O bonds. Although no constraint is imposed on this component, the ratio between the  $\text{C}_3$   
24 area and the normalized area of O 1s peak (not shown here) is always observed between 0.85  
25 and 1.15, which proves the validity of this component. Finally the much broader  $\text{C}_4$  (centered

1 at 290.5 eV, FWHM = 2.8 eV), is assigned to carbon shake up. Whatever the depth analysed,  
2 this component represents about 14.0 % of the C<sub>1</sub> one which corresponds to the amount of  
3 shake up generally observed in literature.

4 These results show that several carbon nitride compounds are created during the  
5 simultaneous implantation of C and N ions into copper. Moreover, the atomic concentration  
6 of each carbon and nitrogen component can be deduced from their areas. Figure 2 shows the  
7 carbon (solid circles) and nitrogen (solid squares) depth profiles obtained by XPS. The  
8 agreement between NRA and XPS carbon depth profiles is very good, even if the XPS one is  
9 slightly broader and less intense due to the decreasing of the XPS depth resolution with  
10 etching time. The carbon retained dose deduced from the XPS results is equal to  
11  $5.4 \cdot 10^{17}$  at.cm<sup>-2</sup>, which is in very good agreement with the carbon retained dose measured by  
12 NRA. However, the nitrogen depth profile obtained by XPS is strongly different from that  
13 obtained by NRA. The nitrogen retained dose is evaluated to be  $1.3 \cdot 10^{17}$  at.cm<sup>-2</sup> whereas we  
14 have found  $4.5 \cdot 10^{17}$  at.cm<sup>-2</sup> by NRA. The precipitation of nitrogen into gas bubbles during the  
15 implantation can explain this strong divergence. Indeed, the gas bubbles will burst during the  
16 etching process. A large part of nitrogen will then be released in the XPS chamber and only a  
17 certain fraction is analyzed. The nitrogen retained dose without the contribution of gas  
18 bubbles was found to be  $0.9 \cdot 10^{17}$  at.cm<sup>-2</sup>. We can then conclude that only 20 % of the  
19 implanted nitrogen interacts with carbon atoms to produce carbon nitride compounds.

20

21

## 22 **4. Conclusion**

23

24 Simultaneous implantation of carbon and nitrogen into copper was performed at  
25 250 °C. Carbon and nitrogen depth profiles were measured using NRA and XPS. The results



1 obtained by NRA were compared and confirmed by SRIM2003. The very good agreement  
2 between the results obtained by NRA and XPS for carbon proves the reliance of the XPS  
3 depth profiling method. The carbon retained dose deduced from both techniques corresponded  
4 to the implanted one. That allowed us to conclude that any diffusion processes during the  
5 implantation are marginal. The long tail observed for higher binding energies in the C 1s core  
6 level spectra revealed the presence of C—N and C—O bonds, but no clear peak components  
7 can be resolved in these spectra. On the other hand the decomposition of N 1s core level  
8 spectra shown that at least two kinds of carbon nitride compounds were formed during the  
9 implantation. Unfortunately the majority of implanted nitrogen atoms precipitate in large gas  
10 bubbles and only about 20 % of them take part in the formation of carbon nitride compounds.

11

12

## 1 **References**

- 2 [1] K.M. Yu, M.L. Cohen, E.E. Haller, W.L. Hansen, A.Y. Liu, I.C. Wu, Phys. Rev. B **49**  
3 (1994) 5034.
- 4 [2] L. Maya, D.R. Cole, E.W. Hagaman, J. Am. Ceram. Soc. **74** (1991) 1686.
- 5 [3] C.M. Niu, Y.Z. Lu, C.M. Lieber, Science **261** (1993) 334.
- 6 [4] E. Gyorgy, V. Nelea, I.N. Mihailescu, A. Perrone, H. Pelletier, A. Cornet, S. Ganatsios,  
7 J. Werckmann, Thin Solid Films **388** (2001) 93.
- 8 [5] A. Hoffman, I. Gouzman, R. Brener, Appl. Phys. Lett. **64** (1994) 845.
- 9 [6] E.A. Romanovsky, O.V. Bespalova, A.M. Borisov, N.G. Goryaga, V.S. Kulikauskas,  
10 V.G. Sukharev, V.V. Zatekin, Nucl. Instr. Meth. B **139** (1998) 355.
- 11 [7] T. Thome, J.L. Colaux, G. Terwagne, Nucl. Instr. Meth. B **249** (2006) 377.
- 12 [8] L. Mayer, SIMNRA, a Simultaiton Program for the Analysis of NRA, RBS and ERDA,  
13 Proc. 15th Int. Conf. Appl. Accelerators in Research and Industry, J. L. Duggan and I.  
14 L. Morgan (eds.), AIP Conf. Proc. **475** (1999) 541.
- 15 [9] M. Kokkoris, P. Misaelides, S. Kossionides, C. Zarkadas, A. Lagoyannis, R. Vlastou,  
16 C.T. Papadopoulos, A. Kontos, Nucl. Instr. Meth. B **249** (2006) 77.
- 17 [10] S. Pellegrino, L. Beck, P. Trouslard, Nucl. Instr. Meth. B **219-20** (2004) 140.
- 18 [11] J.L. Colaux, T. Thome, G. Terwagne, Nucl. Instr. Meth. B **254** (2007) 25.
- 19 [12] T. Thome, J.L. Colaux, J.F. Colomer, G. Bertoni, G. Terwagne, Mater. Chem. Phys. **103**  
20 (2007) 290.
- 21 [13] J.F. Ziegler, J.P. Biersack, U. Littmark, The Stopping and Range of Ions in Solids,  
22 Pergamon, New York, 1967.
- 23 [14] J.L. Colaux, G. Terwagne, Nucl. Instr. Meth. B **240** (2005) 429.
- 24 [15] N. Hellgren, J.H. Guo, Y. Luo, C. Sathe, A. Agui, S. Kashtanov, J. Nordgren, H. Agren,  
25 J.E. Sundgren, Thin Solid Films **471** (2005) 19.

- 1 [16] B. Angleraud, N. Mubumbila, P.Y. Tessier, V. Fernandez, G. Turban, *Diam. Relat. Mat.*  
2 **10** (2001) 1142.
- 3 [17] T. Ujvári, A. Kolitsch, A. Toth, M. Mohai, I. Bertoti, *Diam. Relat. Mat.* **11** (2002) 1149.
- 4 [18] C. Palacio, C. Gomez-Aleixandre, D. Diaz, M.M. Garcia, *Vacuum* **48** (1997) 709.
- 5 [19] A. Nilsson, O. Bjorneholm, H. Tillborg, B. Hernnas, R.J. Guest, A. Sandell, R.E.  
6 Palmer, N. Martensson, *Surf. Sci.* **287** (1993) 758.
- 7  
8  
9  
10

1 Table 1: Energies and calculated ( $R_{SRIM}$ ) and experimental ( $R_{exp}$ ) projected ranges of  $CN^+$ ,  
 2  $^{13}C^{n+}$  and  $^{14}N^{q+}$  ions implanted into copper with a terminal voltage of 400 kV on  
 3 our Tandetron accelerator. As the CN molecule is broken hitting the surface of  
 4 copper sample, the projected range of  $^{13}C^{14}N^+$  corresponds to average of the ones  
 5 of  $^{13}C$  at 401 keV and  $^{14}N$  at 432 keV.  
 6

	E (keV)	$R_{SRIM}$ (nm)	$R_{exp}$ (nm)
$^{13}C^{14}N^+$	833	429	440
$^{13}C$	208	257	280
$^{13}C^+$	608	606	650
$^{13}C^{2+}$	1008	866	910
$^{14}N$	225	240	260
$^{14}N^+$	625	550	600
$^{14}N^{2+}$	1025	775	820

7

8

1 **Figure captions**

2

3 Figure 1: Experimental and simulated NRA spectra recorded at 150° (NRA detector) for the  
4 copper sample simultaneously implanted with  $^{13}\text{C}$  and  $^{14}\text{N}$  at 250°C. Symbols  
5 represent the experimental spectrum and black line represents the simulation  
6 realized with SIMNRA code. Notations of C and N peaks are explained in the text.

7

8 Figure 2: Concentration depth distributions of carbon and nitrogen calculated from  
9 SIMNRA (open symbols) and CASAXPS (solid symbols) simulations for the  
10 copper sample simultaneously implanted with  $^{13}\text{C}$  and  $^{14}\text{N}$  at 250°C.

11

12 Figure 3: XPS depth profile of the multilayered sample (C<sub>50 nm</sub> / Cu<sub>250 nm</sub> / Si) prepared by  
13 physical vapour deposition.

14

15 Figure 4: N 1s (a) and C 1s (b) XPS spectra at a 630 nm depth for the copper sample  
16 implanted with  $^{13}\text{C}$  and  $^{14}\text{N}$  at 250 °C. Experimental data are represented by short  
17 dot lines. Solid lines are the results of the curve fitting Gaussian-Lorentzian  
18 components and the sum of them. Meaning of N<sub>i</sub> and C<sub>i</sub> notations is discussed in  
19 the text.

20

21

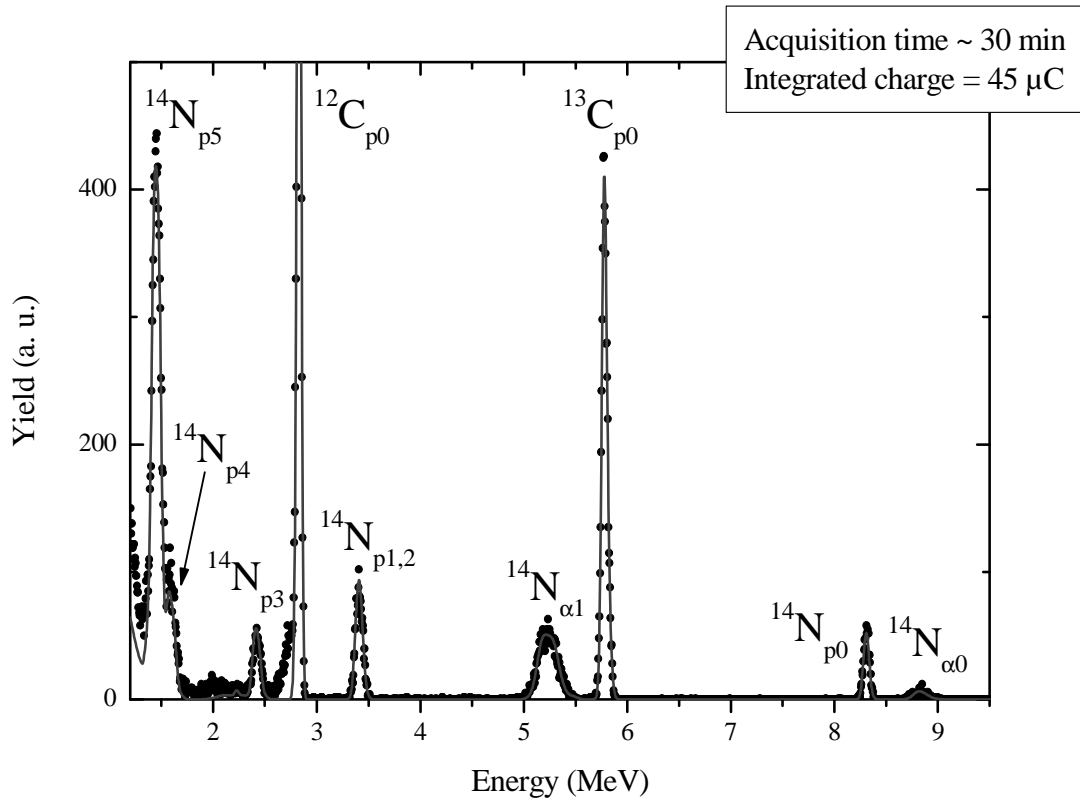
22

23

24

25

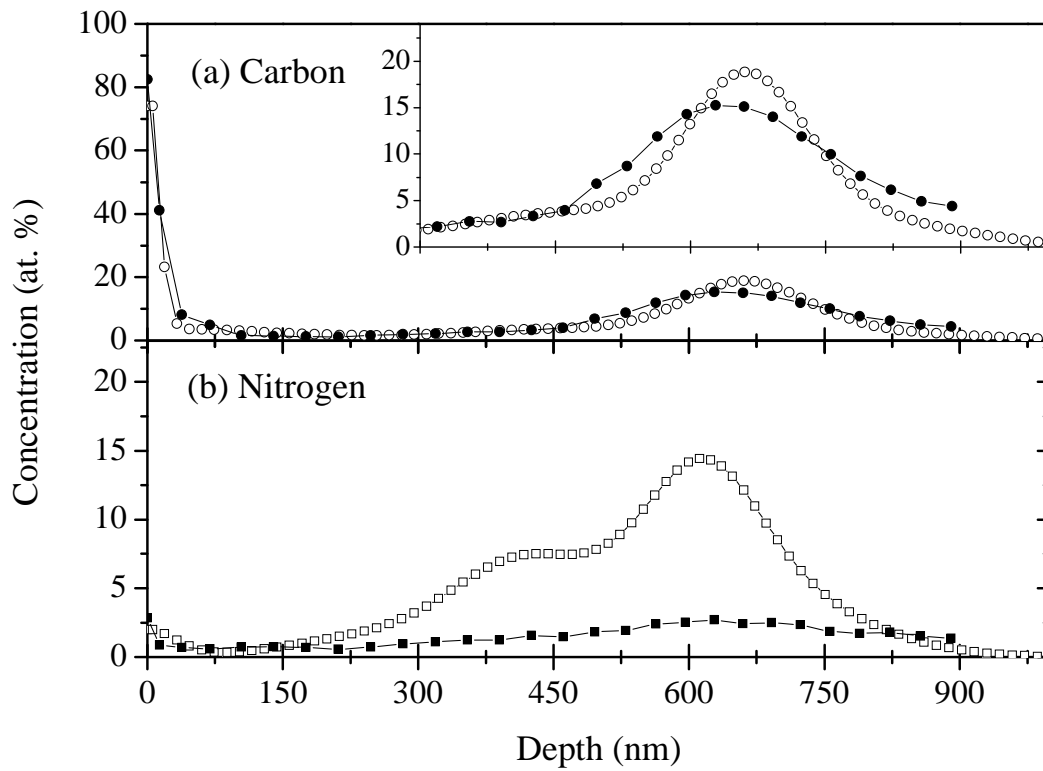
26



1

2

Figure 1



3  
4

Figure 2

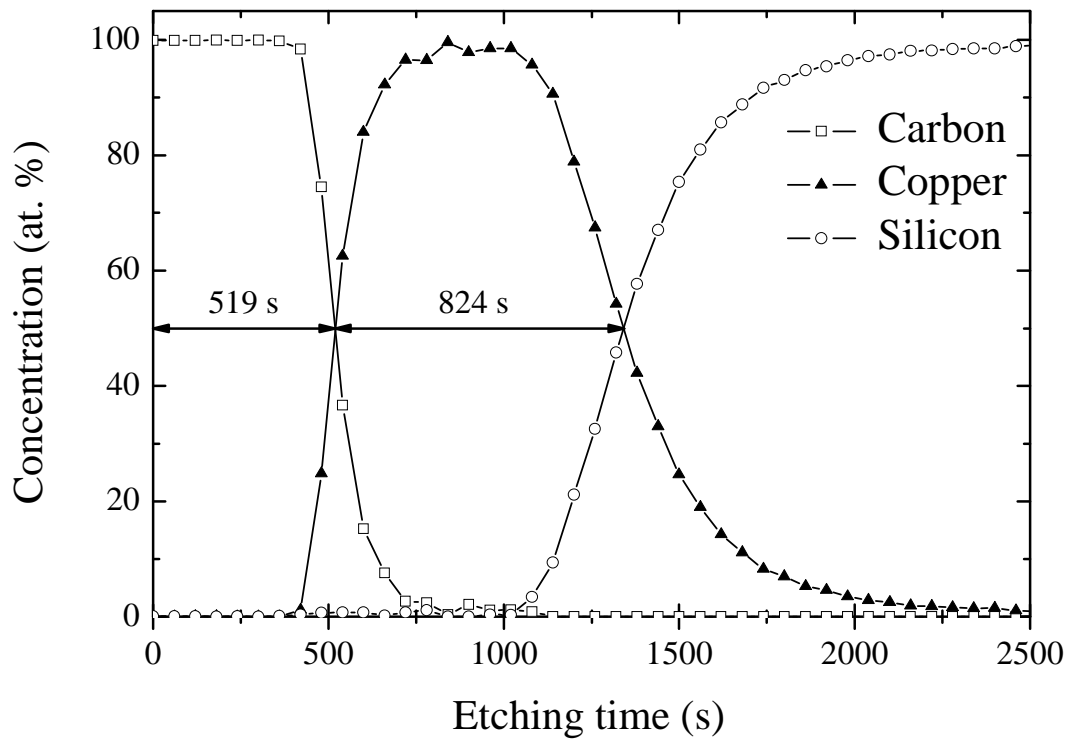


Figure 3

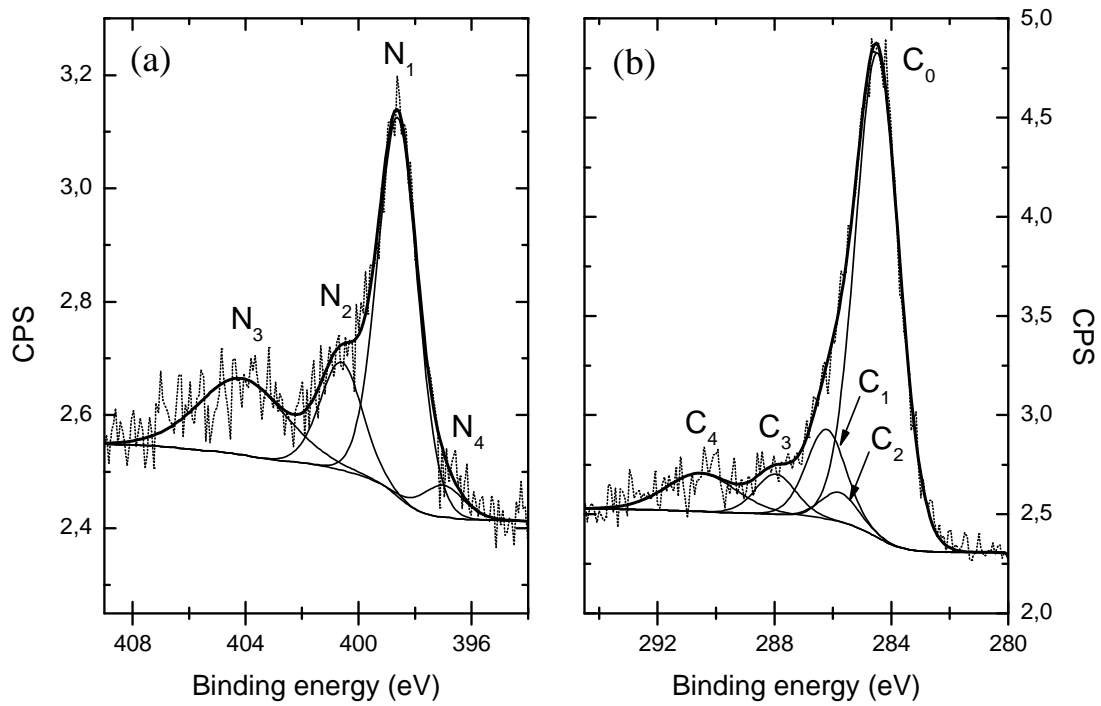


Figure 4

1  
2  
3

4  
5  
6  
7